Sensors and Actuators B 196 (2014) 676–681

Contents lists available at ScienceDirect

Sensors and Actuators B: Chemical

journal homepage: www.elsevier.com/locate/snb

Artificial bacterial flagella functionalized with temperature-sensitive liposomes for controlled release[☆]

Famin Qiu[a], Rami Mhanna[b,1], Li Zhang[c,d], Yun Ding[a], Satoshi Fujita[e,f], Bradley J. Nelson[a,*]

[a] Institute of Robotics and Intelligent System, ETH Zurich, Zurich CH-8092, Switzerland
[b] Cartilage Engineering + Regeneration, ETH Zurich, Zurich CH-8093, Switzerland
[c] Department of Mechanical and Automation Engineering, The Chinese University of Hong Kong, Hong Kong SAR, China
[d] Shenzhen Research Institute, The Chinese University of Hong Kong, Shenzhen, China
[e] Laboratory of Biosensors and Bioelectronics, ETH Zurich, Zurich CH-8092, Switzerland
[f] Biomedical Research Institute, AIST, 1-1-1 Higashi, Tsukuba, Ibaraki 305-8566, Japan

ARTICLE INFO

Article history:
Received 16 September 2013
Received in revised form 28 January 2014
Accepted 29 January 2014
Available online 14 February 2014

Keywords:
Artificial bacterial flagella (ABFs)
Swimming microrobots
Temperature-sensitive liposomes
DPPC
Triggered release

ABSTRACT

Inspired by flagellar propulsion of bacteria such as *E. coli*, artificial bacterial flagella (ABFs) are magnetic swimming microrobots with helical shapes. ABFs are capable of performing precise three-dimensional (3D) navigation in fluids under low-strength rotating magnetic fields making them attractive tools for targeted drug delivery. Further biomedical functionalization of these swimming microrobots is essential to enhance their biological and medical performances. We report the successful functionalization of titanium-coated ABFs with temperature-sensitive dipalmitoylphosphatidylcholine (DPPC)-based liposomes, known as "smart" drug carriers. Liposome coating on the surface of ABFs was confirmed using quartz crystal microbalance with dissipation monitoring (QCM-D) and fluorescent probes. The functionalized ABFs (f-ABFs) showed the ability to incorporate both hydrophilic and hydrophobic drugs. Finally, thermally triggered release of calcein (a common drug analog) from f-ABFs was demonstrated. These f-ABFs have the potential to be used in targeted and triggered drug delivery, microfluidic devices and biosensing.

1. Introduction

Magnetic micro/nanorobots, wirelessly powered by magnetic fields, have the potential to be used in biological and medical applications such as *in vitro* cell manipulation, targeted therapy and *in vivo* sensing [1–8]. Artificial bacterial flagella (ABFs) are magnetic helical microrobots that use a cork-screw strategy for self-propulsion and are of similar size as real bacteria such as *E. coli* [9–12]. ABFs can be actuated in liquid under weak rotating magnetic fields (1000 times lower than the fields used in MRI systems), which are not harmful to living cells and tissues. Their flagellar propulsion, i.e. cork-screw motion, is a promising approach for *in vivo* applications [13,14].

When the helical body of an ABF rotates by following a rotating magnetic field in liquid, the rotational motion translates to translational motion. By changing the rotational axis of the rotating magnetic field, the ABFs swim in 3-D allowing them to precisely target the desired sites. Previous work showed that ABFs can be used to manipulate cellular and sub-cellular objects by direct pushing [15,16] and non-contact methods (agitating the peripheral liquid when an ABF is rotating) [17,18]. However, for biomedical applications such as drug delivery and wireless sensing, further surface biofunctionalization with specific chemicals, such as drug molecules and chemicals, is required [19]. For example, biological modification of the surfaces of nano/micro motors has been used in DNA separation and drug delivery applications [2].

Liposomes have been extensively studied in various applications including drug delivery systems and cell membrane science [20–22]. A liposome is a lipid vesicle consisting of a self-assembled lipid bilayer in which DNA, drugs and/or chemicals can be encapsulated. Liposomes range in size from 20 nm to several hundred micrometers. Depending on the lipid composition of liposomes, their payload can be locally and remotely trigger-released by different stimuli, such as enzymes, pH, ultrasound, light and temperature [23]. Temperature-sensitive liposomes have been proposed for local hyperthermia treatments in cancer therapy [24,25]. Dipalmitoylphosphatidylcholine (DPPC) is commonly used as the key component for temperature-sensitive liposomes. DPPC has a phase

☆ Selected Paper Presented at The 17th International Conference on Solid-State Sensors, Actuators and Microsystems, June 16–20, 2013, Barcelona, Spain.

* Corresponding author. Tel.: +41 44 632 55 29.
E-mail addresses: rami.mhanna@hest.ethz.ch (R. Mhanna), bnelson@ethz.ch (B.J. Nelson).
[1] Tel: +351 253 510913.

0925-4005/$ – see front matter © 2014 Elsevier B.V. All rights reserved.
http://dx.doi.org/10.1016/j.snb.2014.01.099

transition temperature of 41 °C, at which liposomes switch from the solid phase to the liquid-gel phase and become leaky releasing their encapsulated cargo [26]. Adding small amounts of lysolipids (such as 10% 1-myristoyl-2-stearoyl-sn-glycero-3-phosphocholine (MSCP)) with DPPC liposomes increases the drug release rate of DPPC liposomes at 39–42 °C [27,28].

In this work, functionalized ABFs surface-coated with DPPC-based liposomes are reported. Quartz crystal microbalance with dissipation monitoring (QCM-D) was used to investigate the adsorption of liposomes onto a TiO_2 surface. Confocal laser scanning microscopy (CLSM) was used to detect fluorescently labeled (liposome membrane lipids are fluorescent) or calcein loaded (liposome encapsulated calcein is fluorescent) liposomes on the surface of ABFs. Finally, the calcein release from functionalized ABFs was studied.

2. Materials and methods

2.1. Materials

The photoresist IP-L was purchased from Nanoscribe GmbH, Germany. Dipalmitoylphosphatidylcholine (DPPC), 1-myristoyl-2-stearoyl-sn-glycero-3-phosphocholine (MSPC) and lissamine rhodamine B lipids were purchased from Avanti Polar Lipids, Inc. Sodium chloride (NaCl), calcein disodium salt and 4-(2-hydroxyethyl)piperazine-1-ethanesulfonic acid (HEPES) were purchased from Sigma–Aldrich Chemie GmbH, Buchs, Switzerland. The HEPES buffer solution was prepared with 10 mM 4-(2-hydroxyethyl)-1-piperazineethanesulfonic acid and 0.15 M sodium chloride in Milli-Q water (Milli-Q gradient A10, Millipore, resistivity 18.3 MΩ cm). The pH of the buffer was adjusted to pH 7.4 by a 6 M NaOH solution.

2.2. Fabrication process of ABFs

ABF arrays were fabricated using direct laser writing (DLW) and e-beam deposition methods. The process consisted of three steps (Fig. 1): Step 1, writing helical structures in a photoresist IP-L using DLW based on two-photon polymerization [29]; Step 2, developing the written sample in isopropyl alcohol (IPA) to remove un-polymerized resist; Step 3, coating the sample with Ni and then Ti layers (25 nm Ni and 15 nm Ti) using electron beam deposition.

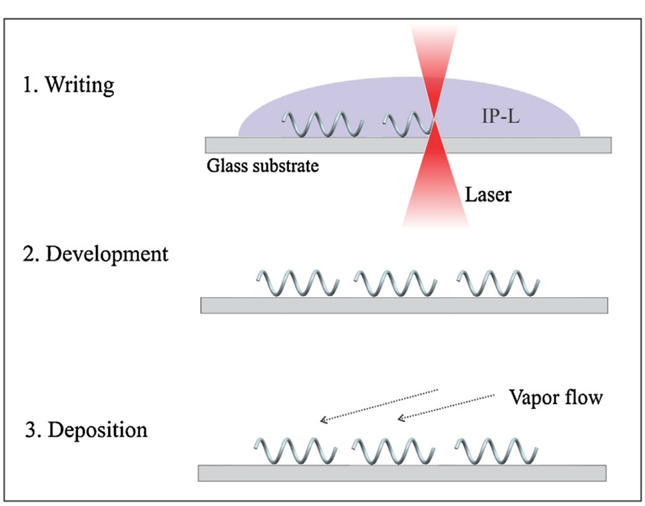

Fig. 1. Fabrication flow of ABFs. Step 1: Writing helical arrays in IP-L photoresist. Step 2: Development in IPA. Step 3: Coating the Ni/Ti bilayer using electron beam deposition.

The Ti layer is naturally oxidized to TiO_2 when exposed to oxygen. A more detailed fabrication process is described elsewhere [15].

2.3. Preparation of liposome-coated ABFs

Fig. 2 shows the three-part preparation flow of liposome-coated ABFs. First, unilamellar DPPC liposomes are prepared. Second, the ABF suspension is prepared, and third, the mixture of the two suspensions and washing generates functionalized ABFs (f-ABFs).

The unilamellar DPPC liposomes were prepared by extrusion [30,31]. DPPC lipids in chloroform were completely dried in a glass vial under a gentle N_2 flow for 30 min and rehydrated with HEPES buffer. In this step, fluorescent molecules can be dissolved in the HEPES buffer to be incorporated within the liposomes. The glass vial was subsequently vortexed to create multilamellar vesicles. The multilamellar vesicle suspension was transferred into a glass syringe and assembled to form the extruder (Fig. S1a). The lipid solution was extruded 31 times through two packed polystyrene membranes (Fig. S1b) to form uniform-sized (200 nm) unilamellar vesicles. Extra care was taken to keep the entire extruder system including the lipid solution above the transition temperature (41 °C) during the extrusion by pre-warming the system at 65 °C in an oven. The DPPC/MSPC (9:1 w/w) was prepared by adding 10% MSPC lipids in DPPC lipids before drying. All lipid mixtures were dissolved in buffer at 2.5 mg/ml concentration.

The second step was to prepare the ABF suspension. The ABF array was cleaned in an UV/ozone cleaner for 30 min followed by washing with Milli-Q water. The array was then detached from the

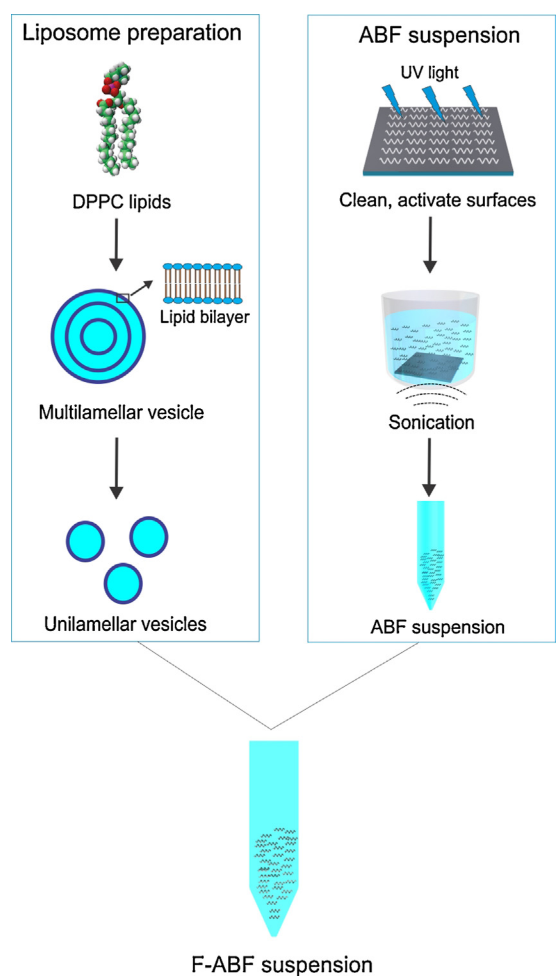

Fig. 2. Preparation flow for coating ABFs with unilamellar DPPC liposomes.

original substrate by sonication in 1 ml HEPES buffer for 2–10 min under 45 kHz, until all ABFs were released from the substrate. After that, the ABFs were pipetted out to a new centrifuge tube. The ABFs were collected in the bottom of the tube by centrifugation (4000 rpm, 3 min) and the volume of the suspension was reduced to 400 μl.

The last step was to prepare f-ABFs. The liposome suspension (100 μl) and ABF suspension (400 μl) were mixed and incubated for enough time (determined by QCM-D) with gentle rotation to obtain a saturated adsorption of liposomes on ABF surfaces, so the final concentration of lipids in the mixture was 0.5 mg/ml.

2.4. QCM-D measurement

Lipids can form a range of different structures on a solid surface including monolayers, intact vesicles or lipid bilayers [32]. In this study the goal was to coat ABFs with intact vesicles which allow entrapment of water-soluble drugs inside the vesicles and/or lipid-soluble drugs within the membrane lipid bilayer. QCM-D is a commonly used tool to measure adsorption of lipids and their structure on surfaces [33]. Lipids adsorbing on the surface of a QCM-D crystal cause a drop in the measured resonant frequency and an increase in the dissipation of the crystal. By monitoring frequency and dissipation changes, the structure, mass and viscoelastic properties of adsorbed lipids can be determined.

Since the surface of ABFs is TiO_2, QCM-D quartz crystals coated with Ti oxidized to TiO_2 were used to simulate the adsorption of DPPC liposomes on ABFs. The crystals were treated equally to the ABF arrays by UV/ozone cleaning for 30 min, followed by washing with Milli-Q water. After the crystal was assembled in the QCM-D (Q-Sense E4, Gothenburg, Sweden) chamber, HEPES buffer was injected into the cell and left until a stable baseline was observed. The liposome solution (0.5 mg/ml) was then injected, and the changes of frequency and dissipation were recorded to monitor the adsorption and stability of lipids on the crystal surface. After the signal response reached a plateau, buffer was injected three times to determine the stability of the adsorbed liposomes. The QCM-D experiment was repeated three times ($n = 3$).

2.5. Confocal laser scanning microscope (CLSM)

In order to confirm the coating of liposomes on ABFs, fluorescent probes, calcein or rhodamine B, were incorporated with liposomes. Calcein (50 mM in HEPES) was entrapped inside the liposomes. Rhodamine B-labeled lipids were incorporated in the liposome lipid bilayer by adding 2% (w/w) to the DPPC initial lipid solution. The f-ABFs were centrifuged (4000 rpm, 3 min) and washed at least five times with HEPES buffer to remove unbound liposomes from the suspension. Images of f-ABFs were taken by a CLSM (Carl Zeiss AG/LSM 510, equipped with a 40 × 0.6 NA objective). The calcein signal was detected using a 488 nm excitation laser and a 505–550 nm band-pass filter. For rhodamine B the laser wavelength was 561 nm, and the filter was BP 575-615 IR.

2.6. Calcein release measurement

Calcein release measurements were performed using DPPC/MSPC (9:1 w/w) liposomes, since this lipid combination has been shown to result in better triggered-release at 41 °C than pure DPPC liposomes [28]. The calcein release from DPPC/MSPC functionalized ABFs (f-ABFs) was qualitatively monitored by CLSM. The fabricated suspensions of f-ABFs were divided equally into three parts and heated at 33, 37 and 41 °C for 1 h, respectively. The fluorescence signals from three samples were recorded by CLSM using the same parameters. In order to obtain quantitative data, the calcein release was measured on a Tecan Infinite M200 PRO plate reader by measuring the fluorescence intensity at the excitation wavelength of 490 nm and emission wavelength of 520 nm. Ti (15 nm) coated Si wafers 5 mm × 5 mm were used to simulate an ABF surface. The wafers were cleaned in UV/ozone cleaner for 30 min, and then incubated with liposomes for 3 h, followed by washing in HEPES buffer 5 times. The wafer was then placed in a 24-well plate containing 1 ml HEPES buffer. The plate was inserted in a plate reader (Tecan Infinite M200 PRO), and the fluorescent intensities were measured at 33, 35, 37, 39 and 41 °C. The temperature was kept constant under each condition for 1 h before measuring. The maximum release of calcein was determined by adding 2% Triton X-100 in HEPES buffer to dissolve the vesicles adsorbed on the wafer. The maximum release was used as the positive control, and the wafer without calcein-loaded liposomes was set as the negative control. The calcein release efficiency was calculated using Eq. (1)

$$\text{Calceinrelease\%} = [(I_{\text{DPPC/MSPC}} - I_{\text{Negative}})/(I_{\text{Positive}} - I_{\text{Negative}})] \times 100, \quad (1)$$

where $I_{\text{DPPC/MSPC}}$, I_{Negative} and I_{Positive} are the fluorescent intensities of the DPPC/MSPC coated wafer, negative control and positive control, respectively [34].

3. Results and discussion

The structure of ABFs was analyzed using scanning electron microscopy (SEM) and adsorption of liposomes was assessed using QCM-D. Fig. 3 shows an SEM image of horizontal ABF arrays, where the length of a single ABF is 16 μm and the diameter is 5 μm. Fig. 4 shows the QCM-D results of DPPC lipids on TiO_2-coated crystals. The data presented were measured at the third overtone. The frequency decreased 414 ± 12 Hz while the dissipation increased up to $48 \pm 3 \times 10^{-6}$ in the first 30 min and reached a plateau after 2 h. This signal is typical of the adsorption of intact liposomes and is consistent with previous reported results [32,33,35]. There was no significant change in the frequency or dissipation after washing the crystal three times with HEPES buffer, which suggests that DPPC liposomes were stable on the TiO_2 surface. For coating DPPC liposomes on the surface of ABFs, we incubated liposomes with ABFs for 3 h to ensure a saturated adsorption.

QCM-D results showed a stable adsorption of DPPC liposomes on the flat surface of the crystal, these results were confirmed using CLSM (Fig. 5). In order to confirm the adsorption of liposomes on 3D-shaped ABFs, rhodamine B labeled lipids (red) were used as a model for a lipid-soluble drug. The rhodamine B-tagged lipids are

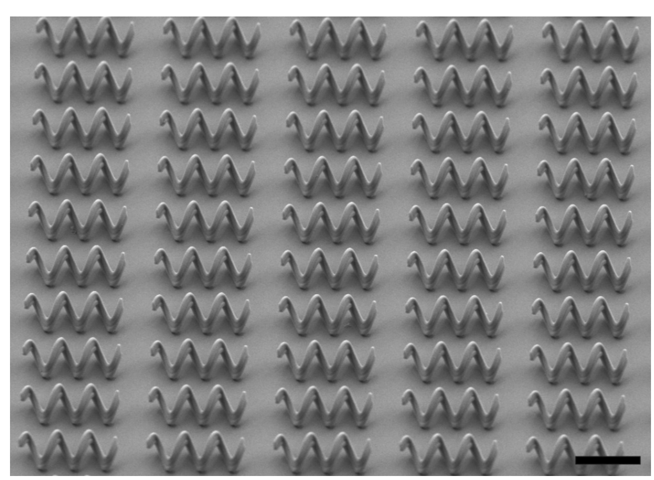

Fig. 3. SEM image of an ABF array taken by the SE2 detector. The scale bar is 10 μm.

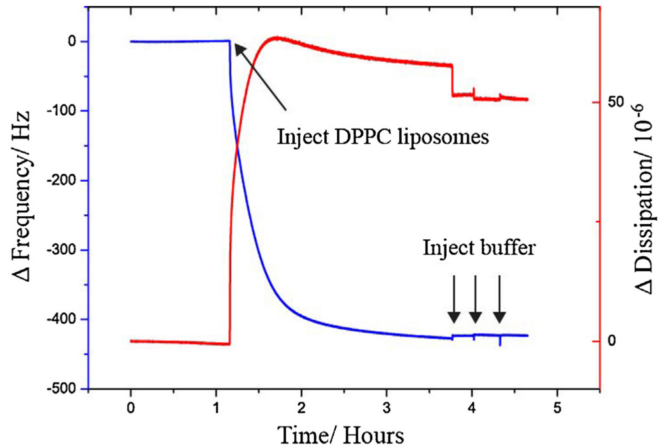

Fig. 4. QCM-D signals in response to the adsorption of DPPC liposomes on a TiO_2 crystal. The blue and red curves are signals of frequency and dissipation of the crystal, respectively. All data presented were measured at the third overtone. (For interpretation of the references to color in this figure legend, the reader is referred to the web version of the article.)

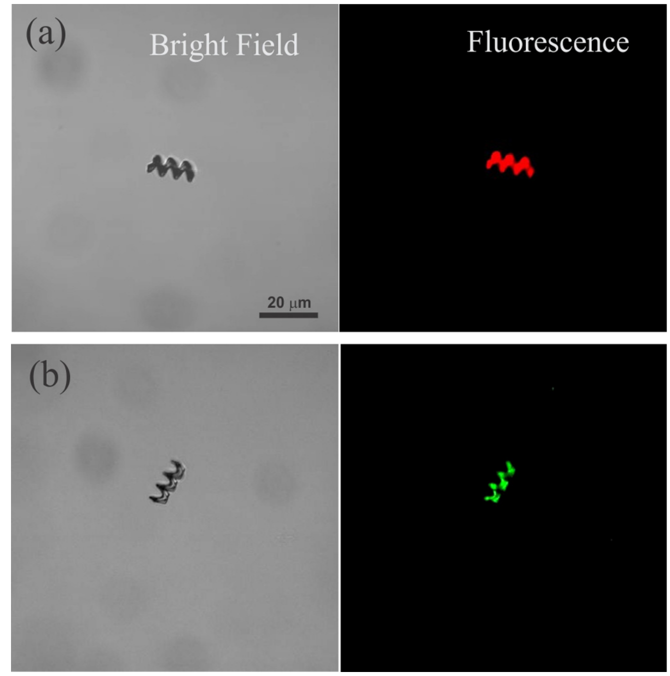

Fig. 5. Fluorescent images of DPPC-coated ABFs. (a) An f-ABF with rhodamine B labeled liposomes. (b) An f-ABF with calcein loaded liposomes.

embedded within the liposome lipid bilayer. Calcein, a green dye, was entrapped within liposomes, mimicking a water-soluble drug. Fig. 5 shows CLSM images of f-ABFs. We used uncoated ABFs as controls to calibrate the intensity of the laser ensuring that any obtained signal was a result of the fluorescent dye and not caused by autofluorescence. Strong signals from both rhodamine B (Fig. 5a, and supporting video S1 shows the 3D image reconstruction of the rhodamine B labeled ABF) and calcein (Fig. 5b) show that liposomes were bound to the ABF surface, which confirms the QCM-D data. This shows that both hydrophobic and hydrophilic drugs can be incorporated in liposomes. The release of the trapped drugs can be temperature-triggered [36]. Furthermore, the fluorescent signal may provide a way to track f-ABFs when they are swimming.

Fig. 6 shows colored-fluorescent images of f-ABFs at 33, 37 and 41 °C, respectively, and the original quantitatible grayscale images of fluorescence are shown in Fig. S2a. The upper three images in Fig. 6 show the fluorescent images and the lower three images show the corresponding overlay images of fluorescence and bright fields. In the upper image of Fig. 6, it can be seen that the fluorescent signals from the f-ABFs hardly changed from 33 to 37 °C, which is due to the saturated fluorescent signals on f-ABFs, while the background signals slightly increased from 33 to 37 °C, which indicates the calcein on the background increased due to the release of calcein from f-ABFs. On the other hand, the fluorescent signals on f-ABFs dramatically decreased from 37 to 41 °C and the background signals increased accordingly, which demonstrates that entrapped calcein was released from the DPPC/MSPC liposomes significantly at 41 °C. By measuring the intensity changes of

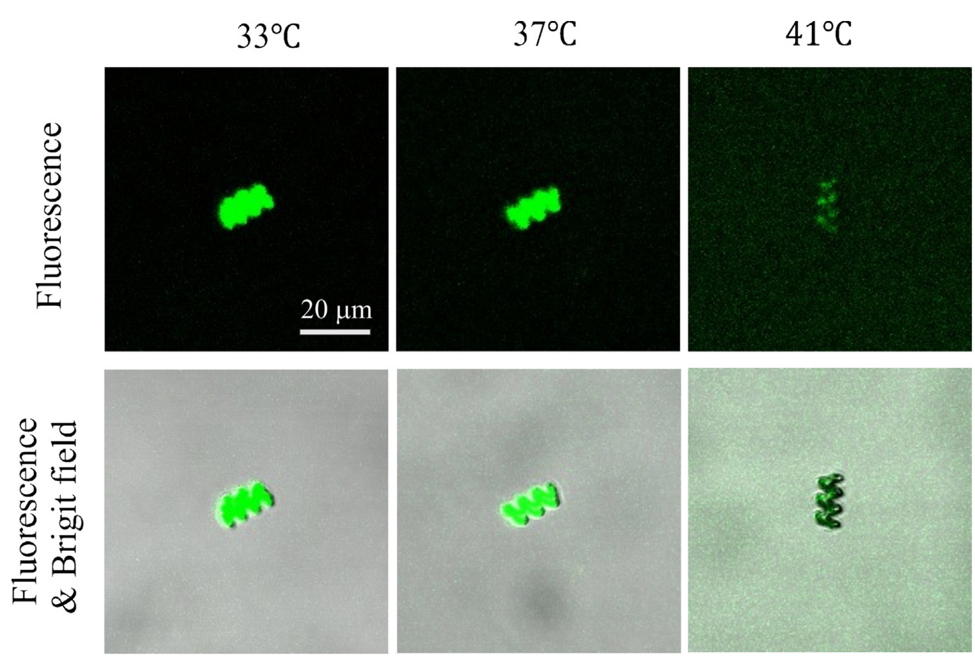

Fig. 6. Calcein release from DPPC/MSPC functionalized ABFs at 33, 37 and 41 °C, respectively. The upper three pictures are fluorescence images, and the lower three pictures are the combined images of fluorescence and bright fields.

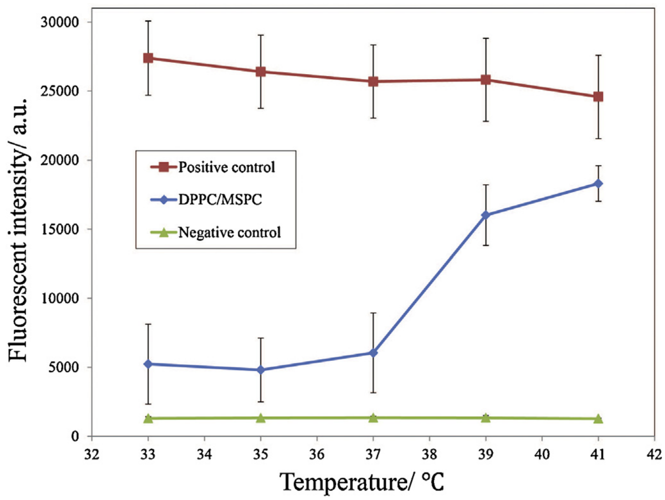

Fig. 7. Calcein release from DPPC/MSPC functionalized TiO_2-coated wafer surfaces. The "DPPC/MSPC" represents the sample coated with DPPC/MSPC liposomes. The "Positive control" represents the liposome-coated sample washed with 2% Triton X-100 in HEPES buffer. The "Negative control" represents the surface without liposome coating. The error bars represent the standard deviations of the values of four measuring points in the well.

the background fluorescence and the f-ABFs on each image using ImageJ software, we roughly calculated the calcein remaining on f-ABFs, which was less than 32% at 41 °C, meaning that the calcein release from f-ABFs at 41 °C was more than 68% (Fig. S2).

For quantitative and precise detection of calcein release from f-ABFs, the preparation of a large number of f-ABFs capturing calcein is required. Because it is technically difficult to obtain these large numbers of f-ABFs and because of errors in the number of ABFs in each experimental set, we used 5 mm × 5 mm Ti coated Si wafers to simulate the calcein release from f-ABFs. The surface area of Ti-coated Si (25 mm^2) is equal to the total surface areas of more than 9000 ABFs, which makes the experiment easier and the total release much higher thus more reliable in quantification. Fig. 7 shows the calcein release from Ti-coated Si wafer measured at 33, 35, 37 and 41 °C. The fluorescent intensity increased dramatically from 37 to 39 °C, which shows that calcein started to burst out from liposomes around 39 °C and continually released till 41 °C. The release efficiency of calcein at 41 °C was 73 ± 15%, calculated according to Eq. (1). This quantity was consistent with the amount of calcein release from f-ABFs at 41 °C (more than 68%) (Fig. S2c).

4. Conclusion

ABFs were successfully functionalized with temperature-sensitive DPPC-based liposomes. Functionalization was confirmed by QCM-D and CLSM results. These f-ABF systems can be wirelessly controlled by low-strength rotating magnetic fields. They show the ability to load both hydrophilic and hydrophobic drugs, and to release calcein (a drug model). The results show calcein was released at 39 °C, and the release efficiency of calcein reached 73 ± 15% at 41 °C. These hybrid systems of ABFs and "smart" carriers can be utilized for targeted delivery and triggered-release of drugs, genes, enzymes and other relevant chemicals for biomedical applications.

Acknowledgements

We would like to thank Prof. Janos Vörös, Kaori Sugihara and Benjamin Simona from the Laboratory of Biosensors and Bioelectronics for their valuable scientific input and discussions and introduction to QCM-D. We thank Prof. Marcy Zenobi-Wong and Christopher Millan from the Cartilage Engineering + Regeneration in ETH Zurich for their scientific input and introduction to CLSM. We also thank Stefano Fusco and Salvador Pané i Vidal from IRIS in ETH Zurich for help with the Tecan Infinite M200 PRO plate reader, Soichiro Tottori for his useful suggestions on preparing Fig. 2, and also the FIRST lab in ETH Zurich for technical support. Funding for this research was provided by the Swiss National Science Foundation (SNSF) Project No. 200021-130069 and the National Natural Science Funds of China (NSFC) for Young Scholar with the Project No. 61305124.

Appendix A. Supplementary data

Supplementary data associated with this article can be found, in the online version, at http://dx.doi.org/10.1016/j.snb.2014.01.099.

References

[1] B.J. Nelson, I.K. Kaliakatsos, J.J. Abbott, Microrobots for minimally invasive medicine, Annu. Rev. Biomed. Eng. 12 (2010) 55–85.
[2] J. Wang, W. Gao, Nano/microscale motors: biomedical opportunities and challenges, ACS Nano 6 (2012) 5745–5751.
[3] T. Petit, L. Zhang, K.E. Peyer, B.E. Kratochvil, B.J. Nelson, Selective trapping and manipulation of microscale objects using mobile microvortices, Nano Lett. 12 (2012) 156–160.
[4] L. Zhang, T. Petit, K.E. Peyer, B.J. Nelson, Targeted cargo delivery using a rotating nickel nanowire, Nanomed. NBM 8 (2012) 1074–1080.
[5] K.B. Yesin, P. Exner, K. Vollmers, B.J. Nelson, Design and control of in-vivo magnetic microrobots, in: J.S. Duncan, G. Gerig (Eds.), Med. Image Comput. Comput. Assist. Intervent. MICCAI (Pt 1) (2005) 819–826.
[6] S. Floyd, C. Pawashe, M. Sitti, Two-dimensional contact and noncontact micromanipulation in liquid using an untethered mobile magnetic microrobot, IEEE Trans. Robot. 25 (2009) 1332–1342.
[7] L. Zhang, J.J. Abbott, L. Dong, K.E. Peyer, B.E. Kratochvil, H. Zhang, et al., Characterizing the swimming properties of artificial bacterial flagella, Nano Lett. 9 (2009) 3663–3667.
[8] S. Tottori, L. Zhang, K.E. Peyer, B.J. Nelson, Assembly, disassembly, and anomalous propulsion of microscopic helices, Nano Lett. 13 (2013) 4263–4268.
[9] L. Zhang, J.J. Abbott, L.X. Dong, B.E. Kratochvil, D. Bell, B.J. Nelson, Artificial bacterial flagella: Fabrication and magnetic control, Appl. Phys. Lett. 94 (2009) 064107.
[10] H.C. Berg, R.A. Anderson, Bacteria swim by rotating their flagellar filaments, Nature 245 (1973) 380–382.
[11] E.M. Purcell, Life at low Reynolds number, Am. J. Phys. 45 (1977) 3–11.
[12] F. Qiu, L. Zhang, K.E. Peyer, M. Casarosa, A. Franco-Obregon, H. Choi, et al., Noncytotoxic artificial bacterial flagella fabricated from biocompatible ORMOCOMP and iron coating, J. Mater. Chem. B 2 (2014) 357–362.
[13] J.J. Abbott, K.E. Peyer, M.C. Lagomarsino, L. Zhang, L.X. Dong, I.K. Kaliakatsos, et al., How should microrobots swim? Int. J. Robot. Res. 28 (2009) 1434–1447.
[14] K.E. Peyer, S. Tottori, F. Qiu, L. Zhang, B.J. Nelson, Magnetic helical micromachines, Chem. A Eur. J. 19 (2013) 28–38.
[15] S. Tottori, L. Zhang, F. Qiu, K.K. Krawczyk, A. Franco-Obregón, B.J. Nelson, Magnetic helical micromachines: fabrication, controlled swimming, and cargo transport, Adv. Mater. 24 (2012) 811–816.
[16] K.E. Peyer, L. Zhang, B.J. Nelson, Bio-inspired magnetic swimming microrobots for biomedical applications, Nanoscale 5 (2013) 1259–1272.
[17] K.E. Peyer, L. Zhang, B.J. Nelson, Localized non-contact manipulation using artificial bacterial flagella, Appl. Phys. Lett. 99 (2011).
[18] L. Zhang, K.E. Peyer, B.J. Nelson, Artificial bacterial flagella for micromanipulation, Lab Chip 10 (2010) 2203–2215.
[19] F. Qiu, L. Zhang, S. Tottori, K. Marquardt, K. Krawczyk, A. Franco-Obregon, et al., Bio-inspired microrobots, Mater. Today 15 (2012) 463.
[20] D. van Swaay, A. deMello, Microfluidic methods for forming liposomes, Lab Chip 13 (2013) 752–767.
[21] M. Bally, K. Bailey, K. Sugihara, D. Grieshaber, J. Vörös, B. Städler, Liposome and lipid bilayer arrays towards biosensing applications, Small 6 (2010) 2481–2497.
[22] M.E. Lynge, M. Baekgaard Laursen, L. Hosta-Rigau, B.E.B. Jensen, R. Ogaki, A.A.A. Smith, et al., Liposomes as drug deposits in multilayered polymer films, ACS Appl. Mater. Interfaces 5 (2013) 2967–2975.
[23] S. Bibi, E. Lattmann, A.R. Mohammed, Y. Perrie, Trigger release liposome systems: local and remote controlled delivery? J. Microencap. 29 (2012) 262–276.
[24] A.M. Ponce, Z. Vujaskovic, F. Yuan, D. Needham, M.W. Dewhirst, Hyperthermia mediated liposomal drug delivery, Int. J. Hyperther. 22 (2006) 205–213.
[25] D. Needham, M.W. Dewhirst, The development and testing of a new temperature-sensitive drug delivery system for the treatment of solid tumors, Adv. Drug Deliv. Rev. 53 (2001) 285–305.
[26] T. Tagami, M.J. Ernsting, S.-D. Li, Optimization of a novel and improved thermosensitive liposome formulated with DPPC and a Brij surfactant using a robust in vitro system, J. Control. Release 154 (2011) 290–297.

[27] R.R. Sawant, V.P. Torchilin, Liposomes as 'smart' pharmaceutical nanocarriers, Soft Matter 6 (2010) 4026–4044.
[28] J.K. Mills, D. Needham, Lysolipid incorporation in dipalmitoylphosphatidylcholine bilayer membranes enhances the ion permeability and drug release rates at the membrane phase transition, Biochim. Biophys. Acta Biomembr. 1716 (2005) 77–96.
[29] Y.-L. Zhang, Q.-D. Chen, H. Xia, H.-B. Sun, Designable 3D nanofabrication by femtosecond laser direct writing, Nano Today 5 (2010) 435–448.
[30] F. Olson, C.A. Hunt, F.C. Szoka, W.J. Vail, D. Papahadjopoulos, Preparation of liposomes of defined size distribution by extrusion through polycarbonate membranes, Biochim. Biophys. Acta 557 (1979) 9–23.
[31] R.C. Macdonald, R.I. Macdonald, B.P.M. Menco, K. Takeshita, N.K. Subbarao, L.R. Hu, Small-volume extrusion apparatus for preparation of large, unilamellar vesicles, Biochim. Biophys. Acta 1061 (1991) 297–303.
[32] N.-J. Cho, C.W. Frank, B. Kasemo, F. Höök, Quartz crystal microbalance with dissipation monitoring of supported lipid bilayers on various substrates, Nat. Protocols 5 (2010) 1096–1106.
[33] E. Reimhult, F. Hook, B. Kasemo, Intact vesicle adsorption and supported biomembrane formation from vesicles in solution: Influence of surface chemistry, vesicle size, temperature, and osmotic pressure, Langmuir 19 (2003) 1681–1691.
[34] M. Afadzi, C.d.L. Davies, Y.H. Hansen, T. Johansen, Ø.K. Standal, R. Hansen, et al., Effect of ultrasound parameters on the release of liposomal calcein, Ultrasound Med. Biol. 38 (2012) 476–486.
[35] A. Fortunelli, S. Monti, Simulations of lipid adsorption on TiO_2 Surfaces in Solution, Langmuir 24 (2008) 10145–10154.
[36] D. Felnerova, J.F. Viret, R. Gluck, C. Moser, Liposomes and virosomes as delivery systems for antigens, nucleic acids and drugs, Curr. Opin. Biotechnol. 15 (2004) 518–529.

Biographies

Famin Qiu earned his Bachelor's degree from the Department of Materials Science and Engineering, Ocean University of China, Qingdao, in 2008, and the M.E. degree from the Department of Materials Science and Engineering, Zhejiang University, Hangzhou, China, in 2011. In May 2011, he joined the Institute of Robotics and Intelligent Systems at ETH Zürich as a Ph.D. student, and his research interests include micro-/nanodevices and their biomedical applications.

Rami Mhanna received his BE in computer and communications engineering from Notre Dame University (Zouk Mosbeh, Lebanon) in 2006 and his MSc in biomedical engineering from The University of Melbourne (Melbourne, Australia) in 2008. He pursued his doctoral studies in the Biosensors and Bioelectronics and the Cartilage Engineering and Regeneration labs at the Swiss Federal Institute of Technology (ETH Zurich, Switzerland). He defended his Ph.D. in 2013 and his research focus is in the fields of tissue engineering and drug delivery.

Li Zhang received the Ph.D. degree from the University of Basel, Switzerland, in 2007. He joined the Institute of Robotics and Intelligent Systems (IRIS), Swiss Federal Institute of Technology (ETH) Zurich, Switzerland, as a postdoc in 2007, and as a senior scientist from 2009 to 2012. He is currently an Assistant Professor in the Department of Mechanical and Automation Engineering and an associate faculty member in the Biomedical Engineering Programme at The Chinese University of Hong Kong. His main research interests include design and fabrication of micro-/nanodevices and their biomedical applications, microfluidics, and nanomaterials for energy storage and environmental applications.

Yun Ding earned his Bachelor's degree in Pharmaceutical Engineering at Zhejiang University, China, in 2009. He received his Master's degree from ETH Zurich in Chemical and Bioengineering in 2012. After that, he joined the Prof. deMello's group as a Ph.D. student in the same Institute so far. His current research interest focuses on developing segmented-flow (or droplet-based) microfluidic systems for high-throughput chemical and biological experimentation.

Satoshi Fujita received a Ph.D. in engineering from University of Tsukuba in 2000. In 2003, he became project assistant professor at The University of Tokyo. Since 2004, he has been working in National Institute of Advanced Industrial Science and Technology (AIST) in Japan as a research scientist (2004–2008) and a senior research scientist (2008–present). His principal research interests lie in the development of cellular nano-device technology combined with nano technology, molecular biology and cell biology.

Brad Nelson received mechanical engineering degrees from the University of Illinois (B.S. 1984) and the University of Minnesota (M.S.1987), and a Ph.D. in Robotics (School of Computer Science) from Carnegie Mellon University (1995). Prof. Nelson has been on the faculty of the University of Minnesota and the University of Illinois at Chicago, has worked at Motorola and Honeywell, and has served as a United States Peace Corps Volunteer in Botswana, Africa. He is the Professor of Robotics and Intelligent Systems at the Swiss Federal Institute of Technology (ETH), Zurich and heads the Institute of Robotics and Intelligent Systems (IRIS).